1521-0111/12/8103-299–308$25.00
MOLECULAR PHARMACOLOGY
Vol. 81, No. 3
74120/3746654

Mol Pharmacol 81:299–308, 2012

AC927, a σ Receptor Ligand, Blocks Methamphetamine-Induced Release of Dopamine and Generation of Reactive Oxygen Species in NG108-15 Cells

Nidhi Kaushal, Meenal Elliott, Matthew J. Robson, Anand Krishnan V. Iyer,[1] Yon Rojanasakul, Andrew Coop, and Rae R. Matsumoto

Department of Basic Pharmaceutical Sciences, School of Pharmacy, West Virginia University Health Sciences Center, Morgantown, West Virginia (N.K., M.E., M.J.R., A.K.V.I., Y.R., R.R.M.); and Department of Pharmaceutical Sciences, School of Pharmacy, University of Maryland, Baltimore, Maryland (A.C.)

Received June 17, 2011; accepted November 18, 2011

ABSTRACT

Methamphetamine is a highly addictive psychostimulant drug of abuse that causes neurotoxicity with high or repeated dosing. Earlier studies demonstrated the ability of the selective σ receptor ligand *N*-phenethylpiperidine oxalate (AC927) to attenuate the neurotoxic effects of methamphetamine in vivo. However, the precise mechanisms through which AC927 conveys its protective effects remain to be determined. With the use of differentiated NG108-15 cells as a model system, the effects of methamphetamine on neurotoxic endpoints and mediators such as apoptosis, necrosis, generation of reactive oxygen species (ROS) and reactive nitrogen species (RNS), and dopamine release were examined in the absence and presence of AC927. Methamphetamine at physiologically relevant micromolar concentrations caused apoptosis in NG108-15 cells. At higher concentrations of methamphetamine, necrotic cell death was observed. At earlier time points, methamphetamine caused ROS/RNS generation, which was detected with the fluorigenic substrate 5-(and-6)-chloromethyl-2′,7′-dichlorodihydrofluorescin diacetate, acetyl ester, in a concentration- and time-dependent manner. *N*-Acetylcysteine, catalase, and L-N^G-monomethyl arginine citrate inhibited the ROS/RNS fluorescence signal induced by methamphetamine, which suggests the formation of hydrogen peroxide and RNS. Exposure to methamphetamine also stimulated the release of dopamine from NG108-15 cells into the culture medium. AC927 attenuated methamphetamine-induced apoptosis, necrosis, ROS/RNS generation, and dopamine release in NG108-15 cells. Together, the data suggest that modulation of σ receptors can mitigate methamphetamine-induced cytotoxicity, ROS/RNS generation, and dopamine release in cultured cells.

Introduction

Methamphetamine (METH) is a highly abused psychostimulant drug that results in neurotoxicity with high or repeated drug administration (Krasnova and Cadet, 2009). This neurotoxicity is seen as dopamine nerve terminal degeneration and apoptosis in several brain regions (Krasnova and Cadet, 2009), the mechanism of which is not completely understood. However, some of the neurotoxic cascades involved are excessive release of dopamine, oxidative/nitrosative stress, endoplasmic reticulum (ER) stress, and activation of mitochondrial death cascades (Cadet and Brannock, 1998; Krasnova and Cadet, 2009).

Among its various targets, METH interacts with σ receptors at physiologically relevant micromolar concentrations (Nguyen et al., 2005; Han and Gu, 2006). Two subtypes of σ receptors, σ_1 and σ_2, are expressed in almost all types of mammalian cells (Guitart et al., 2004). σ_1 Receptors are

This work was supported by the National Institutes of Health National Institute on Drug Abuse [Grant DA 013978].

Portions of this work were presented in abstract form: Matsumoto RR, Elliott M, Kaushal N, Iyer AKV, Rojanasakul Y, Coop A, AC927, a selective sigma receptor ligand, blocks the generation of reactive oxygen species induced by methamphetamine in NG108-15 cells (program 727.3), Neuroscience 2010; 11–12 Nov 2010, San Diego, CA. Society for Neuroscience, Washington DC.

[1]Current affiliation: School of Pharmacy, Hampton University, Hampton, Virginia.

Article, publication date, and citation information can be found at http://molpharm.aspetjournals.org.

http://dx.doi.org/10.1124/mol.111.074120.

ABBREVIATIONS: AC927, *N*-phenethylpiperidine oxalate; ANOVA, analysis of variance; CM-H_2DCFDA, 5-(and-6)-chloromethyl-2′,7′-dichlorodihydrofluorescin diacetate, acetyl ester; DAT, dopamine transporter; DMEM, Dulbecco's modified Eagle's medium; DMSO, dimethylsulfoxide; ER, endoplasmic reticulum; FBS, fetal bovine serum; HAT, hypoxanthine-aminopterin-thymidine; METH, methamphetamine; NAC, *N*-acetylcysteine; L- NMMA, L- N^G-monomethyl arginine citrate; MFI, mean fluorescence intensity; NET, norepinephrine transporter; NO, nitric oxide; NOS, nitric-oxide synthase; PBS, phosphate-buffered saline; PCR, polymerase chain reaction; RNS, reactive nitrogen species; ROS, reactive oxygen species; SERT, serotonin transporter; TEMED, *N*,*N*,*N*′,*N*′-tetramethylethylenediamine; TH, tyrosine hydroxylase.

highly conserved, 223-amino acid, membrane-bound proteins (Kekuda et al., 1996). They function as chaperones at the mitochondria-ER membrane and regulate Ca^{2+} signaling via inositol trisphosphate receptors (Hayashi and Su, 2007). In addition, σ_1 receptors can undergo protein-protein interactions with several other cellular proteins, such as binding immunoglobulin protein, ankyrin-B, inositol trisphosphate receptors, and dopamine D_1 receptors (Hayashi and Su, 2007; Navarro et al., 2010; Su et al., 2010). σ_1 Receptors are also capable of translocation to different subcellular compartments upon stimulation through ligand binding and changes in intracellular conditions (Hayashi and Su, 2003). In contrast, σ_2 receptors are less well characterized. However, their levels are elevated in immortalized cell lines and tumor cells (Vilner et al., 1995), where they have been implicated in the control of cell cycle functions (Wheeler et al., 2000), alterations in cellular Ca^{2+} levels (Vilner and Bowen, 2000), and cell death signaling involving sphingolipid products (Crawford et al., 2002).

Previous in vivo studies showed that pretreatment with *N*-phenethylpiperidine oxalate (AC927), a σ receptor ligand, attenuates the neurotoxic effects of METH in male Swiss-Webster mice (Matsumoto et al., 2008; Seminerio et al., 2011). The ability of AC927 to mitigate neurotoxic cascades is consistent with the location of σ receptors in various subcellular organelles, such as ER, mitochondria, lysosomes, cell membranes, and nuclei (McCann et al., 1994; Zeng et al., 2007), as well as the functional roles of σ receptors in cells, as described above. The role of σ receptors in neurotoxicity resulting from drugs of abuse such as METH remains unclear because of various limitations, including the lack of a suitable in vitro model system. Previous studies on the mechanisms of METH-induced toxicity used either primary neuronal cultures or immortalized cell lines of neuronal origin (Cadet et al., 1997; Wu et al., 2007). Millimolar concentrations of METH were required to induce cell death/damage, but such concentrations are rarely achieved in vivo (Melega et al., 2008). Therefore, a model system suitable for identification of potential mechanisms leading to neurotoxicity is needed.

To elucidate the cellular mechanisms of METH-induced neurotoxicity at which AC927 may intervene via σ receptors, a neuronal/glial cell culture model (neuroblastoma × glioma hybridoma; NG108-15 cells) was used in the present study. When they are differentiated, NG108-15 cells display neurite outgrowth and electrical excitability and express proteins with neuronal and glial properties (Ma et al., 1998). These cells have been used extensively as a sensitive cell line for studies of the toxic effects of various drugs and chemicals (Cañete and Diogène, 2008). In addition, NG108-15 cells have commonly been used to study the functions of σ receptors (Hayashi and Su, 2003). In the current study, the endpoints measured were reactive oxygen species (ROS) and reactive nitrogen species (RNS) generation, dopamine release, apoptosis, and necrosis. Finally, AC927 was tested against these cytotoxic endpoints and mediators for insights into the mechanisms of σ receptor-mediated neuroprotection.

Materials and Methods

Drugs and Chemicals. Phosphate-buffered saline (PBS), Dulbecco's modified Eagle's medium (DMEM), penicillin/streptomycin solution, hypoxanthine/aminopterin/thymidine (HAT), trypsin/EDTA (0.05% trypsin, 0.43 mM EDTA), 5-(and 6)-chloromethyl-2′,7′-dichlorodihydrofluorescein diacetate (CM-H_2DCFDA), dithiothreitol, and TRIzol lysis reagent were obtained from Invitrogen (Carlsbad, CA). Ammonium persulfate, fetal bovine serum (FBS), dimethylsulfoxide (DMSO), methamphetamine-HCl, sodium dichromate, catalase, *N*-acetylcysteine (NAC), L-N^G-monomethyl arginine citrate (L-NMMA), potassium chloride, sodium azide, sodium bichromate, sodium metabisulfite, Trizma base, glycine, Tris-buffered saline with Tween 20, and EDTA were obtained from Sigma-Aldrich Chemicals (St. Louis, MO). Chloroform, hydrogen peroxide, hydrochloric acid, isopropanol, and methanol were purchased from Fisher Scientific (Pittsburgh, PA), and polyacrylamide/bisacrylamide solution (37.5:1; 2.6% cross-linking agent), SDS (20%), and TEMED were purchased from Bio-Rad Laboratories (Hercules, CA). A permeabilization-fixation staining buffer kit was obtained from BD Biosciences (San Jose, CA). AC927 was synthesized in the laboratory of Dr. Andrew Coop (University of Maryland, Baltimore, MD), as described previously (Maeda et al., 2002).

Cell Line and Culture. The neuroblastoma × glioma hybridoma cell line NG108-15 was obtained from American Type Culture Collection (Manassas, VA). Cells were maintained at 37°C in 25-cm^2 (T25) or 75-cm^2 (T75) culture flasks (Costar; Corning Life Sciences, Lowell, MA), in high-glucose (4.5 g/l) DMEM supplemented with 10% FBS, penicillin, streptomycin, and HAT, in a humidified incubator with 5% CO_2. When cells were 70% confluent in the flasks, the medium was replaced with differentiation medium (DMEM with 0.5% FBS, penicillin, streptomycin, HAT, and 1% DMSO) and cells were allowed to differentiate for an additional 2 to 4 days before being harvested for dopamine assays, flow cytometry, and quantitative real-time PCR studies. For ROS assays, cells were plated in complete medium in 48-well CellBind tissue culture plates (Corning-Costar), at 2.5×10^4 cells per well, and were allowed to become 80% confluent, whereupon the culture medium was replaced with differentiation medium and the cells were allowed to differentiate for an additional 2 to 4 days. For apoptosis assays, cells were plated in complete medium in BD Falcon black Optilux 96-well plates (BD Biosciences) coated with a mixture of poly-D-lysine and mouse laminin (1 $\mu g/cm^2$ each), at 10^4 cells per well. The medium was replaced with differentiation medium (DMEM with 0.5% FBS, penicillin, streptomycin, HAT, and 1% DMSO) after 24 h, and the cells were allowed to differentiate for an additional 3 to 4 days.

Flow Cytometry. NG108-15 cells grown and differentiated in T75 flasks were harvested and were washed once with PBS containing 1% FBS and 0.09% NaN_3. Cells were fixed and permeabilized for 20 min on ice in permeabilization-fixation buffer, washed with permeabilization-wash buffer, and incubated for 20 min with the primary antibodies chicken anti-σ_1 receptor antibody (amino acids 65–78; LRRLHPGHVLPDEE), nonspecific chicken IgY (Aves Laboratories, Tigard, OR), rabbit anti-tyrosine hydroxylase antibody (AB152), or nonspecific rabbit IgG antibody (amino acids 12–370; Millipore, Billerica, MA), at 1:100 dilution per 10^6 cells. Cells were washed once with permeabilization-wash buffer (BD Biosciences) and were counterstained for 20 min with the following fluorescein isothiocyanate-conjugated secondary antibodies: rabbit anti-chicken antibody or goat anti-rabbit antibody (Southern Biotechnology Associates, Birmingham, AL). Cells were washed in permeabilization-wash buffer once more and were resuspended in PBS containing 1% FBS and 0.09% NaN_3, and data were acquired by using a FACSCaliber system (BD Biosciences). The data were plotted and analyzed by using FCS Software (De Novo Software, Los Angeles, CA). The mean fluorescence intensity (MFI) values for staining in multiple experiments were subjected to statistical analyses.

Real-Time PCR. NG108-15 cells grown and differentiated in T25 flasks, as described above, were harvested, washed once with ice-cold PBS, and resuspended in appropriate extraction buffer. Bilateral striatum samples were dissected from male Swiss-Webster mice, flash-frozen, and stored at −80°C until RNA isolation. RNA isola-

tions were conducted by using TRIzol reagent (Invitrogen), according to the manufacturer's instructions. The quality and quantity of RNA were assessed by using a spectrophotometer (Biochrom, Cambridge, UK). One microgram of RNA was used to synthesize cDNA with Superscript-H cDNA synthesis kits (Applied Biosystems, Foster City, CA); the cDNA was then used as a template for real-time PCR with oligonucleotide primer sets specific for 18S rRNA (Hs99999901_s1), mouse DAT mRNA (Mm00438396_m1), mouse σ_1 receptor mRNA (Mm00448086M1), mouse SERT mRNA (Mm00439391_m1), mouse NET mRNA (Mm00436661_m1), rat NET mRNA (Rn00580207_m1), mouse dopamine D_1 receptor mRNA (Mm01353211_m1), or rat dopamine D_1 receptor mRNA (Rn03062203_s1), with Taqman real-time PCR master mixture (Applied Biosystems), for 45 cycles in a StepOnePlus real-time PCR system (Applied Biosystems). The difference in cycles to threshold for each sample was recorded by using 18S as an endogenous control. The threshold was set at 0.2 for all genes tested. The change in the difference in cycles to threshold method was used to calculate relative quantities of each gene in NG108-15 cells, compared with mouse or rat striatum samples.

ROS Assays. Cells grown in complete medium or differentiation medium were used for assays when 60% to 70% confluent. The culture medium was replaced with 200 μl of phenol red-free medium containing 0.5% FBS and 5 μM levels of the fluorigenic oxidizable dye CM-H_2DCFDA, and cells were returned to the incubator at 37°C for 45 to 60 min. Cells were gently rinsed once with phenol red-free medium and were fed with 200 μl of the same medium and appropriate concentrations of METH or AC927, ranging from 0 to 300 μM. Exogenously added 100 μM H_2O_2 served as a positive control in this assay. Also included was 100 μM $Na_2Cr_2O_7$, a well known source of carcinogenic chromium VI (O'Brien et al., 2003), which was shown previously to induce ROS in human lung cancer cells (Azad et al., 2008). All compounds were added in replicates of 4 or 8, and the plates were returned to the incubator. In some assays, AC927 was added 15 min before the addition of METH, $Na_2Cr_2O_7$, or H_2O_2. Inhibitors of ROS were added at the same time as the dye before the addition of METH, $Na_2Cr_2O_7$, or H_2O_2 and again after rinsing of the cells to remove remaining extracellular dye and before the addition of METH. At specified time points, plates were read in a Fluostar Optima fluorescence plate reader fitted with a 485/520-nm excitation/emission filter set (BMG Labtech, Offenberg, Germany). Data were obtained as relative fluorescence units after background subtraction. In some assays, relative fluorescence unit values for untreated controls for each assay were averaged and the values for each treated sample were normalized with respect to that average, followed by statistical analyses.

Dopamine Quantitation. NG108-15 cells grown and differentiated in T75 flasks were harvested through replacement of the medium with Ca^{2+}/Mg^{2+}-free Dulbecco's PBS, centrifuged, resuspended in differentiation medium with reduced glucose (1.5 g/l) at 3×10^5 cells per ml, and seeded in 24-well CellBind tissue culture plates at 0.5 ml per well. After 4 h, various concentrations of METH (0–300 μM) were added to sets of wells. KCl (50 mM) was used as a positive control for maximal dopamine release. In one set of wells, AC927 (0.3 μM) was added 15 min before the addition of METH or KCl. After 5 min of exposure to KCl or METH, supernatants were harvested (450 μl), centrifuged to remove cells, and acidified with the addition of 45 μl of buffer (0.1 N HCl, 10 mM EDTA, 40 mM $Na_2S_2O_5$), and samples were stored at −20°C. Dopamine levels were quantitated by using an enzyme-linked immunosorbent assay kit from Rocky Mountain Diagnostics (Denver, CO), with the manufacturer's protocols. Dopamine was extracted from the culture supernatants through binding to an affinity gel matrix, acetylated, eluted, and then measured by using an ultrasensitive, competition, enzyme-linked immunosorbent assay and a standard curve with known concentrations of dopamine.

Apoptosis and Necrosis Assays. NG108-15 cells were grown and differentiated in 96-well plates. On the day of the experiment, the culture medium was replaced with 100 μl of phenol red-free differentiation medium. The cells were pretreated with AC927 (0–30 μM) 15 min before treatment with various concentrations of METH (0–1 mM) for 24 h at 37°C. Hoechst 33342 stain (20 μg/ml; Invitrogen) and propidium iodide (Invitrogen) were added to the wells, and the plate was incubated at room temperature for 10 min. After the incubation step, the plate was placed under the microscope with UV light, and 2 or 3 pictures per well were taken by using Leica Application Suite imaging software (Leica Microsystems, Buffalo Grove, IL). Cells that were stained bright blue and displayed fragmented nuclei were counted as apoptotic, and cells that were red were counted as necrotic. The proportions of apoptotic and necrotic cells were calculated by using ImageJ software (http://rsbweb.nih.gov/ij/).

Statistical Analyses. Statistical analyses of data included *t* tests and analysis of variance (ANOVA) with appropriate post hoc tests, using Prism 4 (GraphPad Software, San Diego, CA).

Results

Differentiated NG108-15 Cells Express σ_1 Receptors and Tyrosine Hydroxylase. Figure 1A shows representative histograms from flow cytometric detection of the σ_1 receptor and tyrosine hydroxylase (TH) in fixed and permeabilized NG108-15 cells. Staining using chicken anti-σ_1 receptor and rabbit anti-TH antibodies was found in single peaks with MFI values of 38.24 ± 2.52 and 39.60 ± 2.87, respectively, whereas the control antibodies chicken IgY and rabbit IgG detected peaks with MFI values (arbitrary units) of 3.35 ± 0.08 and 3.30 ± 0.09, respectively, which represented background staining. Statistical analysis, with unpaired *t* tests, of

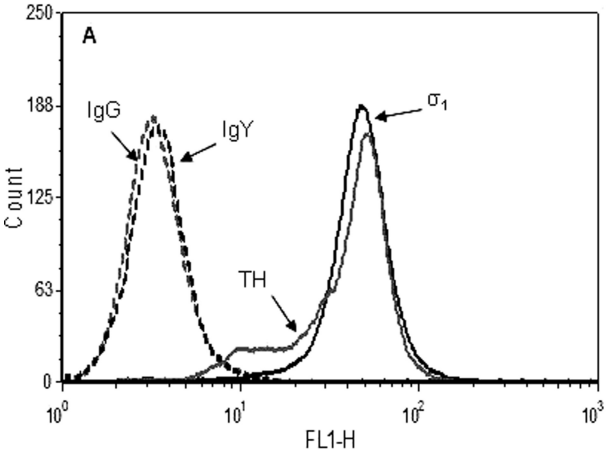

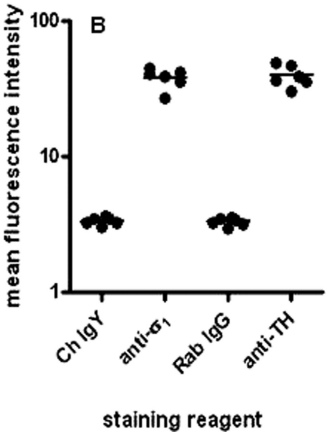

Fig. 1. Expression of σ_1 receptors and TH in NG108-15 cells. A, representative histograms from six independent experiments. NG108-15 cells were fixed, permeabilized, stained, and analyzed as described under *Materials and Methods*. Histograms are as follows: control chicken IgY (dashed black), chicken anti-σ_1 receptor (solid black), control rabbit IgG (dashed gray), and rabbit anti-TH (solid gray) antibodies. FL1-H (*x*-axis), fluorescence channel height; counts (*y*-axis), number of events detected for the corresponding fluorescence channel. B, MFI values for all four stains from six separate experiments plotted against the staining reagent. Ch, chicken; Rab, rabbit.

results obtained in six separate experiments (Fig. 1B) confirmed a significant shift in MFI values for antigen-specific staining over background (for σ_1 receptor versus control IgY, $t = 13.80$, $p < 0.0001$; for TH versus control IgG, $t = 12.63$, $p < 0.0001$).

Differentiated NG108-15 Cells Express DAT, SERT, NET, and Dopamine D_1 Receptor mRNA. Table 1 depicts mRNA expression levels for DAT, SERT, NET, dopamine D_1 receptors, and σ_1 receptors in differentiated NG108-15 cells and rat or mouse striatum. Difference in cycles to threshold values, as well as gene fold change ratios for NG108-15 cells with respect to striatum samples, are included. Unpaired two-tailed t tests were used to compare mRNA levels between mouse or rat striatum and differentiated NG108-15 cells. There were significant differences in mRNA expression levels for DAT ($t = 16.95$, $p < 0.0001$), σ_1 receptors ($t = 3.07$, $p < 0.01$), SERT ($t = 5.98$, $p < 0.0001$), and dopamine D_1 receptors (mouse, $t = 47.20$, $p < 0.0001$; rat, $t = 34.73$, $p < 0.0001$). NET was expressed in similar quantities in NG108-15 cells and rat striatum ($t = 0.87$, not significant). Mouse NET was found not to be expressed in differentiated NG108-15 cells.

METH Generates ROS/RNS in Differentiated NG108-15 Cells. As shown in Fig. 2A, CM-H_2DCFDA detected exogenously added H_2O_2 within 10 min (168.91 ± 6.95% of untreated control) and up to 60 min (176.69 ± 7.10% of control). Low levels of ROS were induced in NG108-15 cells by $Na_2Cr_2O_7$ starting at 10 min; ROS levels in this sample increased dramatically 4 h after treatment (140.10 ± 8.60% of control) and continued to increase up to 24 h, reaching 223.70 ± 21.92% of levels in untreated control cells.

All tested concentrations of METH except the lowest (0.1 μM) induced the production of ROS capable of oxidizing CM-H_2DCFDA significantly above background levels within 10 min of exposure, with 3 μM inducing the highest levels (201.97 ± 9.97% of control) (Table 2). The difference between METH-induced ROS levels and basal ROS levels in NG108-15 cells decreased after 60 min, whereas ROS continued to accumulate up to 24 h in cells treated with $Na_2Cr_2O_7$. Statistical analysis of the data obtained from 10 to 60 min by using two-way, repeated-measures ANOVA and Bonferroni's post hoc tests further established that concentrations of METH capable of reproducibly inducing the strongest sustained ROS responses were 1 μM ($p < 0.001$), 3 μM ($p < 0.001$), and 300 μM ($p < 0.001$) concentrations at 10, 20, 30, and 60 min (Table 2).

As shown in Fig. 2B, CM-H_2DCFDA detected exogenously added H_2O_2 within 10 min (146.69 ± 4.97% of control) and ROS generated by $Na_2Cr_2O_7$ in NG108-15 cells, which peaked at 24 h (242.06 ± 11.56% of control). In contrast, all tested concentrations of AC927 from 0 to 300 μM failed to induce ROS levels significantly higher than those in untreated control cells. Statistical analyses of the data by using two-way, repeated-measures ANOVA showed significant effects of AC927 and positive control treatment ($F_{9,900} = 75.37$, $p < 0.0001$), time ($F_{6,900} = 28.36$, $p < 0.0001$), and AC927 and positive control treatment-time interaction ($F[54,900] = 60.50$, $p < 0.0001$). Bonferroni's post hoc tests revealed that none of the tested concentrations of AC927 was able to induce elevation of ROS levels above background levels, whereas ROS was detected in cells treated with H_2O_2 (10 min, $t = 11.26$, $p < 0.001$; 20 min, $t = 14.14$, $p < 0.001$; 30 min, $t = 14.50$, $p < 0.001$; 60 min, $t = 11.47$, $p < 0.001$; 240 min, $t = 3.03$, $p < 0.05$; 480 min, $t = 3.00$, $p < 0.05$) and $Na_2Cr_2O_7$ (240 min, $t = 7.01$, $p < 0.001$; 480 min, $t = 16.52$, $p < 0.001$; 1440 min, $t = 34.24$, $p < 0.001$). AC927 at 0.3 μM led to a reduction in basal ROS levels in NG108-15 cells, with the reduction becoming statistically significant at 240 min ($t = 3.78$, $p < 0.01$), 480 min ($t = 2.87$, $p < 0.05$), and up to 1440 min ($t = 4.38$, $p < 0.001$).

As shown in Fig. 3A, CM-H_2DCFDA-detectable ROS induced in NG108-15 cells by 0.1 to 3 μM METH was completely inhibited in the presence of the common antioxidant and radical scavenger NAC, as seen within 20 min after addition of the drug, which confirms that the assay was detecting ROS (Fig. 3A). One-way ANOVA showed that the inhibition was significant ($F[13,99] = 95.57$, $p < 0.0001$). Bonferroni's post hoc tests with pairwise comparisons showed that NAC induced significant decreases in ROS levels for all tested concentrations of METH ($t = 11.96$–13.64, $p < 0.001$ for all concentrations). Significant inhibition of radical generation persisted up to 4 h after addition of METH, at which time the experiment was terminated. NAC also reduced the levels of ROS detectable in untreated control cells ($t = 7.97$, $p < 0.001$).

The presence of catalase in the assay medium (10,000 units per ml) inhibited ROS induced by 1 and 3 μM METH and detected with CM-H_2DCFDA within 20 min after addition of the drug (Fig. 3B). One-way ANOVA confirmed that the inhibition was significant ($F[11,91] = 7.74$, $p < 0.0001$). Bonferroni's post hoc tests with pairwise comparisons indi-

TABLE 1

mRNA expression levels of receptors and transporters in differentiated NG108-15 cells

Quantitative real-time PCR analysis of expression levels of mRNA for DAT, SERT, NET, dopamine D_1 receptors, and σ_1 receptors in NG108-15 cells, compared with either rat or mouse striatum, was performed. There were significant differences in mRNA expression levels for DAT, σ_1 receptor, SERT, and dopamine D_1 receptor; however, mRNA for NET was expressed in similar quantities in NG108-15 cells and rat striatum. Mouse NET was not expressed in NG108-15 cells. Data shown represent the difference in cycles to threshold values for each gene in NG108-15 cells and mouse or rat bilateral striatum samples, compared with 18S endogenous control. Data are represented as mean ± S.E.M. Gene fold changes were calculated by using the change in difference in cycles to threshold method, and NG108-15/rat or mouse striatum ratios were calculated from those values.

Gene	TaqMan Probe	Difference in Cycles to Threshold			Gene Fold Change Ratio
		NG108-15	Mouse Striatum	Rat Striatum	
Mouse DAT (Slc6a3)	Mm00438396_m1	29.41 ± 0.21***	25.01 ± 0.11	N.D.	0.050
σ_1 receptor	Mm00448086_m1	16.89 ± 0.19**	17.74 ± 0.19	N.D.	1.760
Mouse SERT (Slc6a4)	Mm00439391_m1	25.30 ± 0.17***	26.90 ± 0.22	N.D.	2.953
Mouse NET (Slc6a2)	Mm00436661_m1	N.P.	N.D.	N.D.	
Rat NET (Slc6a2)	Rn00580207_m1	28.71 ± 0.18	N.D.	29.02 ± 0.32	1.144
Mouse dopamine D_1 receptor	Mm01353211_m1	27.05 ± 0.18***	15.34 ± 0.14	N.D.	0.00031
Rat dopamine D_1 receptor	Rn03062203_s1	28.40 ± 0.36***	N.D.	12.81 ± 0.27	0.00002

N.D., not determined; N.P., not present.
**$P < 0.01$, ***$P < 0.0001$, unpaired two-tailed t test.

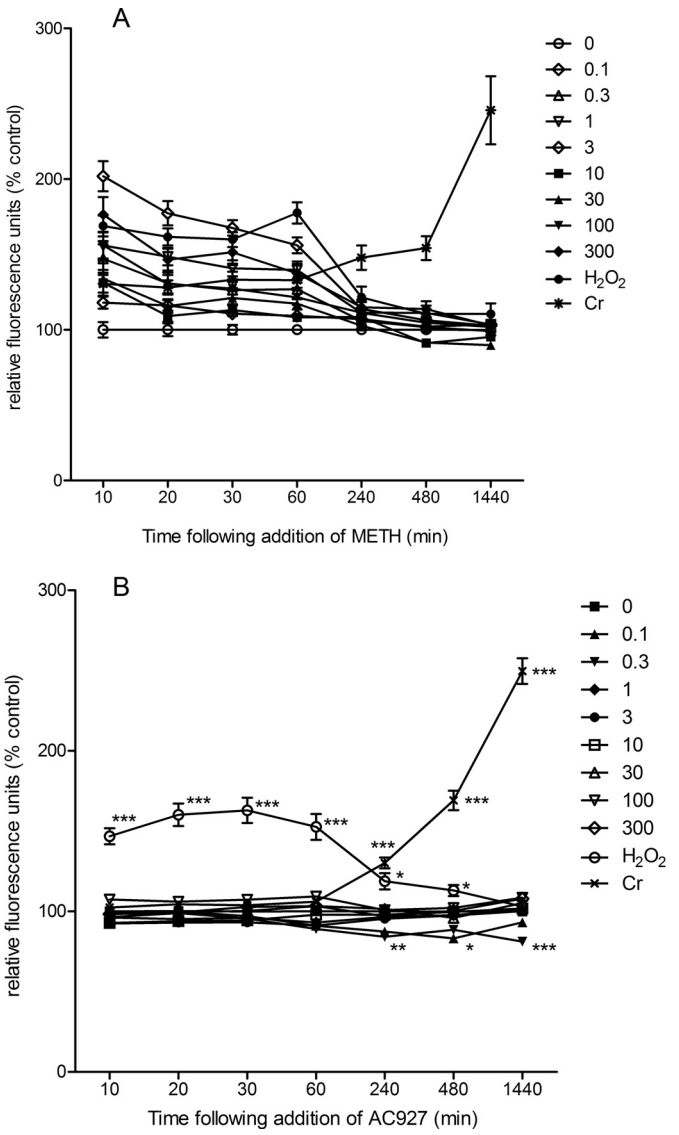

Fig. 2. ROS induced in NG108-15 cells after exposure to METH or AC927. The production of ROS capable of oxidizing CM-H_2DCFDA was conducted as described under *Materials and Methods*, in NG108-15 cells after exposure to 100 μM H_2O_2,100 μM $Na_2Cr_2O_7$ (Cr), or 0 to 300 μM METH (A) or 0 to 300 μM AC927 (B). Relative fluorescence units from five (A) or two (B) separate experiments for each indicated time point are shown; data were normalized to the mean relative fluorescence unit values for untreated cells to obtain percentage of control values ($n = 8$ per experiment; mean ± S.E.M.). *, $p < 0.05$; **, $p < 0.01$; ***, $p < 0.001$, versus control treatment.

cated significant differences with both 1 μM ($t = 3.17$, $p < 0.05$) and 3 μM ($t = 3.20$, $p < 0.05$) METH.

The increase in ROS in NG108-15 cells induced by 1 and 3 μM METH was also significantly inhibited in the presence of L-NMMA; data shown were obtained 20 min after addition of the drug (F[13,83] = 28.41, $p < 0.0001$, one-way ANOVA) (Fig. 3C). Bonferroni's post hoc tests and pairwise comparisons revealed significant changes with both 1 μM ($t = 4.20$, $p < 0.001$) and 3 μM ($t = 4.78$, $p < 0.001$) METH.

AC927 Attenuates METH-Induced ROS/RNS Generation in Differentiated NG108-15 Cells. As shown in Fig. 4, METH caused a significant increase in ROS/RNS generation (F[10,79] = 13.84, $p < 0.0001$). Post hoc Dunnett's tests showed that all concentrations of METH except 30 μM showed significant ROS/RNS generation (0.1 μM, $q = 3.62$, $p < 0.01$; 0.3 μM, $q = 3.42$, $p < 0.01$; 1 μM, $q = 4.44$, $p < 0.01$; 3 μM, $q = 8.30$, $p < 0.01$; 10 μM, $q = 3.63$, $p < 0.01$; 100 μM, $q = 3.42$, $p < 0.01$; 300 μM, $q = 7.39$, $p < 0.01$). AC927 at 0.3 μM attenuated the production of reactive radicals induced by METH, reducing them to levels observed in untreated control cells for all tested concentrations of METH; data shown here were obtained 20 min after stimulation with METH. Two-way ANOVA showed a significant effect of AC927 pretreatment ($F_{1,138} = 98.44$, $p < 0.0001$), METH or positive control treatment (F[10,138] = 15.63, $p < 0.0001$), and AC927 pretreatment-METH or positive control treatment interaction (F[10,138] = 2.39, $p < 0.05$). Bonferroni's post hoc tests showed that AC927 attenuated ROS/RNS generation at the following METH concentrations: 0.1 μM ($t = 3.28$, $p < 0.05$), 0.3 μM ($t = 3.16$, $p < 0.05$), 1 μM ($t = 3.52$, $p < 0.01$), 3 μM ($t = 7.16$, $p < 0.001$), 10 μM ($t = 3.99$, $p < 0.01$), 30 μM ($t = 3.14$, $p < 0.05$), 100 μM ($t = 3.39$, $p < 0.05$), and 300 μM ($t = 3.84$, $p < 0.01$). As expected, AC927 did not inhibit oxidation of the dye by exogenously added H_2O_2 at 20 min ($t = 1.39$, not significant) or at later time points. It also failed to inhibit significantly the small amount of ROS generation produced by $Na_2Cr_2O_7$ at this time point ($t = 0.99$, not significant). At later time points, however, AC927 inhibited ROS induction by $Na_2Cr_2O_7$, as seen at 4 h ($t = 4.05$, $p < 0.001$) and 24 h ($t = 7.73$, $p < 0.001$).

AC927 Attenuates METH-Induced Dopamine Release in Differentiated NG108-15 Cells. As shown in Fig. 5, 0.0 to 41.85 pg of dopamine was detected in untreated cells. In contrast, when cells were treated with KCl, 268.30 to 389.62 pg of dopamine was detected in the culture supernatant 5 min after exposure.

Dopamine release was induced by all four concentrations of METH, ranging from 0.3 to 300 μM, with 3 μM METH inducing maximal release of 204.75 to 413.12 pg per 1.5×10^5 cells, compared with that in untreated control cells (F[5,23] = 8.87, $p < 0.0005$). In cells treated with 0.3, 30, and 300 μM METH, mean values for dopamine levels ranged from 153.00 ± 46.60 to 165.50 ± 27.81 pg per 1.5×10^5 cells. Levels of dopamine released in response to 0.3, 3, and 300 μM METH were significantly above levels in untreated controls (0.3 μM, $q = 2.77$, $p < 0.05$; 3 μM, $q = 5.32$, $p < 0.01$; 300 μM, $q = 2.76$, $p < 0.05$; Dunnett's multiple-comparison tests).

In cells exposed to 0.3 μM AC927 for 5 min, dopamine levels were not significantly different from those in untreated controls (Fig. 5). Preexposure of cells to 0.3 μM AC927 for 15 min before stimulation with METH prevented the release of dopamine (mean values ranging from 8.84 to 32.33 pg per 1.5×10^5 cells). The attenuation of dopamine release by AC927 was statistically significant, as judged by one-way ANOVA (F[11,41] = 13.96, $p < 0.0001$) and Bonferroni's post hoc tests with pairwise comparisons, for the 0.3 μM ($t = 3.19$, $p < 0.05$) and 3 μM ($t = 5.58$, $p < 0.001$) concentrations of METH. Pretreatment of cells with AC927 did not, however, block the release of dopamine in cells treated with KCl ($t = 0.23$, not significant).

AC927 Prevents METH-Induced Apoptosis and Necrosis in Differentiated NG108-15 Cells. The apoptotic effects of various concentrations of METH (0–1 mM) on NG108-15 cells over a period of 24 h are shown in Fig. 6A. One-way ANOVA showed that METH caused a significant, concentration-dependent increase in the proportion of apo-

TABLE 2

Induction of ROS in NG108-15 cells by physiological concentrations of METH

NG108-15 cells were cultured and assayed as described in *Materials and Methods*. Relative fluorescence units for each experimental point (each concentration of METH at distinct time points, 10, 20, 30, and 60 min) were obtained. Values for untreated cells (0 μM METH; $n = 32$) for each assay plate were averaged and set at 100. Values for experimental points were converted to percentage of untreated control values for each assay plate. Data shown are mean ± S.E.M. of percentage of control values ($n = 8$ per experiment) from four separate experiments. Two-way, repeated-measures ANOVA of percentage of control values with Bonferroni's post hoc tests permitted comparison of the effect of time on each of the METH concentrations tested. H_2O_2 and $Na_2Cr_2O_7$ served as positive controls.

	ROS			
	10 min	20 min	30 min	60 min
	% of control			
METH				
0 μM	100.09 ± 5.14	100.05 ± 4.24	100.03 ± 3.26	100.00 ± 2.75
0.1 μM	118.06 ± 4.01	116.22 ± 3.49	110.72 ± 2.89	109.53 ± 2.57
0.3 μM	141.84 ± 9.61***	130.81 ± 7.22**	126.28 ± 5.64*	123.41 ± 6.69*
1 μM	161.28 ± 8.71***	148.56 ± 5.81***	140.78 ± 5.40***	133.94 ± 5.74***
3 μM	201.97 ± 9.97***	177.34 ± 8.04***	167.56 ± 5.18***	147.41 ± 5.10***
10 μM	131.22 ± 8.48**	109.03 ± 3.65	113.03 ± 3.91	107.63 ± 2.86
30 μM	134 ± 11.82***	115.81 ± 4.47	121.03 ± 4.79	115.06 ± 3.77
100 μM	156.09 ± 8.82***	130.38 ± 6.12**	127.25 ± 6.34**	118.38 ± 4.62
300 μM	176.38 ± 11.67***	146.59 ± 7.27***	151.44 ± 8.53***	132.94 ± 5.80***
100 μM H_2O_2	168.91 ± 6.95***	166.34 ± 5.41***	164.63 ± 4.60***	176.69 ± 7.12***
100 μM $Na_2Cr_2O_7$	130.53 ± 5.86**	123.34 ± 3.72*	128.47 ± 4.70**	132.28 ± 5.10**

* $P < 0.05$.
** $P < 0.01$.
*** $P < 0.001$.

ptotic cells ($F_{7,187} = 37.21$, $p < 0.0001$). Post hoc analysis with Dunnett's tests showed that the following concentrations of METH caused significant increases in apoptosis, compared with controls: 3 μM ($q = 2.87$, $p < 0.05$), 10 μM ($q = 3.74$, $p < 0.01$), 100 μM ($q = 5.99$, $p < 0.001$), 300 μM ($q = 7.73$, $p < 0.001$), and 1000 μM ($q = 13.68$, $p < 0.001$).

AC927 pretreatment significantly attenuated the apoptotic effects of METH. Two-way ANOVA showed significant effects of METH treatment ($F_{6,392} = 37.82$, $p < 0.0001$), AC927 pretreatment ($F_{3,392} = 55.94$, $p < 0.0001$), and METH treatment-AC927 pretreatment interaction ($F[18,392] = 5.41$, $p < 0.0001$). Post hoc Bonferroni's tests showed that AC927 (0.3, 3, and 30 μM) attenuated the apoptotic effects of METH. AC927 at 0.3 μM attenuated the apoptotic effects of the following concentrations of METH: 3 μM ($t = 3.34$, $p < 0.01$), 10 μM ($t = 3.70$, $p < 0.01$), 100 μM ($t = 5.05$, $p < 0.001$), 300 μM ($t = 5.85$, $p < 0.001$), and 1000 μM ($t = 9.80$, $p < 0.001$). AC927 at 3 μM prevented the apoptotic effects of the following concentrations of METH: 10 μM ($t = 3.52$, $p < 0.01$), 100 μM ($t = 3.45$, $p < 0.01$), 300 μM ($t = 5.67$, $p < 0.001$), and 1000 μM ($t = 8.84$, $p < 0.001$). AC927 at 30 μM attenuated the apoptotic effects of the following concentrations of METH: 100 μM ($t = 3.20$, $p < 0.05$), 300 μM ($t = 3.00$, $p < 0.05$), and 1000 μM ($t = 7.82$, $p < 0.001$).

The necrotic effects of various concentrations of METH (0–1 mM) on NG108-15 cells over a period of 24 h are shown in Fig. 6B. One-way ANOVA showed that METH caused a significant, concentration-dependent increase in the proportion of necrotic cells ($F_{7,187} = 7.35$, $p < 0.0001$). Post hoc analysis with Dunnett's tests showed that the following concentrations of METH caused significant increases in necrosis, compared with no-treatment controls: 300 μM ($q = 3.82$, $p < 0.01$) and 1000 μM ($q = 5.88$, $p < 0.01$).

AC927 pretreatment significantly attenuated the necrotic effects of METH. Two-way ANOVA showed significant effects of METH treatment ($F_{6,392} = 8.32$, $p < 0.0001$) and AC927 pretreatment ($F_{3,392} = 17.14$, $p < 0.0001$). Post hoc Bonferroni's tests showed that the following concentrations of AC927 attenuated the necrotic effects of METH at 300 and 1000 μM: 0.3 μM, 300 μM METH, $t = 4.33$, $p < 0.001$; 1000 μM METH, $t = 4.26$, $p < 0.001$; 3 μM, 300 μM METH, $t = 3.30$, $p < 0.01$; 1000 μM METH, $t = 3.91$, $p < 0.001$; 30 μM, 300 μM METH, $t = 3.29$, $p < 0.01$; 1000 μM METH, $t = 2.87$, $p < 0.05$.

Discussion

This study showed that METH caused apoptosis in differentiated NG108-15 cells at physiologically relevant micromolar concentrations and could cause necrosis at higher concentrations. At earlier time points, ROS/RNS generation and release of dopamine were also observed. AC927, a σ receptor ligand, attenuated the apoptotic and necrotic cell death as well as the neurotoxicity mediators. The implications of these findings are discussed below.

In the first part of the study, differentiated NG108-15 cells were confirmed to express various receptors and transporters through which METH mediates its effects, including σ_1 and dopamine D_1 receptors; dopamine, serotonin, and norepinephrine transporters; and the synthetic enzyme tyrosine hydroxylase. Extensive studies have corroborated the presence of σ receptors in NG108-15 cells (Vilner et al., 1995; Su et al., 2010). Previous studies also demonstrated the production of dopamine in these differentiated catecholaminergic cells (Ghahary et al., 1989). Collectively, the presence of tyrosine hydroxylase, monoamine transporters, and D_1 receptors suggests a functional dopaminergic neurotransmitter system in these cells. Although the levels of DAT are low in the NG108-15 cell line, higher levels of SERT can compensate through functional reuptake of dopamine released into the synapses (Schmidt and Lovenberg, 1985).

One of the key mediators of METH neurotoxicity is ROS/RNS generation, which can occur through multiple mechanisms, including excessive dopamine release, microglial activation, glutamate release, and mitochondrial dysfunction (Krasnova and Cadet, 2009). Excessive generation of ROS/RNS can injure neurons and surrounding cells through direct oxidative damage to cellular components such as lipids, pro-

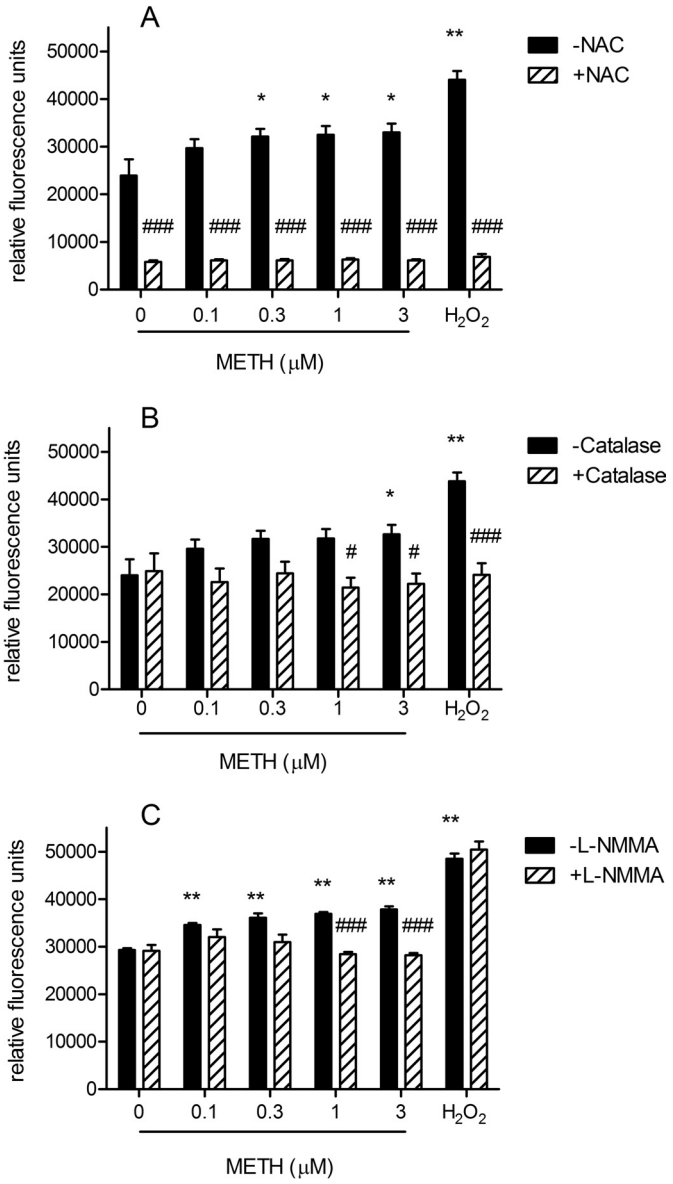

Fig. 3. Inhibition of ROS production in NG108-15 cells by NAC, catalase, and L-NMMA. Inhibition of ROS after exposure to 0 to 3 μM METH or 100 μM H_2O_2 was determined in the absence or presence of 10 mM NAC (A), 10,000 units catalase (B), or 20 mM L-NMMA (C), 20 min after exposure to METH. Data represent the average ± S.E.M. of relative fluorescence units from two separate experiments ($n = 4$ per experiment). *, $p < 0.05$; **, $p < 0.01$, control versus METH-treated; #, $p < 0.05$; ###, $p < 0.001$, METH alone versus METH with ROS inhibitor.

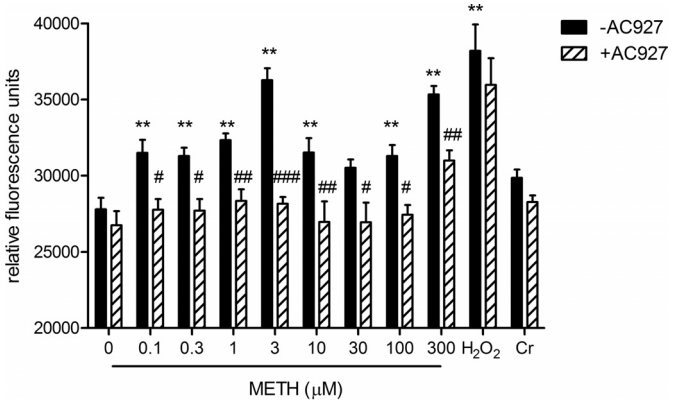

Fig. 4. Inhibition of METH-induced ROS generation in NG108-15 cells by AC927. The production of ROS capable of oxidizing CM-H_2DCFDA was assessed in differentiated NG108-15 cells in the presence of 0 to 300 μM METH, 100 μM H_2O_2, or 100 μM $Na_2Cr_2O_7$ (Cr), in the absence or presence of 0.3 μM AC927, as described under *Materials and Methods*. Data represent the average ± S.E.M. of relative fluorescence units from two different experiments ($n = 8$ per experiment), obtained 20 min after the addition of drug. **, $p < 0.01$, control versus METH-treated; #, $p < 0.05$; ##, $p < 0.01$; ###, $p < 0.001$, METH alone versus METH with AC927.

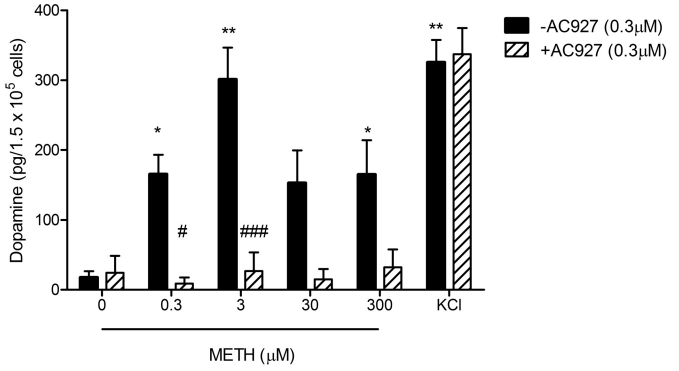

Fig. 5. Release of dopamine from NG108-15 cells in response to METH. Values for supernatants harvested from NG108-15 cells cultured in the presence or absence of METH and/or AC927 (*x*-axis) and quantitated as described under *Materials and Methods* are represented as picograms of dopamine per 1.5 × 10^5 cells in 500 μl of medium. Data represent the mean ± S.E.M. from four (METH or KCl alone) or three (METH with AC927) independent experiments. *, $p < 0.05$; **, $p < 0.01$, control versus METH- or KCl-treated; #, $p < 0.05$; ###, $p < 0.001$, METH alone versus METH with AC927.

teins, and DNA or through ER stress and activation of mitochondrial death cascades, ultimately leading to nerve terminal degeneration or cell death (Krasnova and Cadet, 2009). This study demonstrated that METH generates ROS/RNS in the NG108-15 model system. All tested concentrations of METH ranging from 0.1 to 300 μM induced the production of ROS/RNS within 10 min after exposure. High stable ROS/RNS levels were detected at 20 min and up to 60 min after exposure of NG108-15 cells to METH. The levels of ROS/RNS decreased after the first hour, which indicates that the cells may shift to the production of radicals not detected by CM-H_2DCFDA. Alternatively, in METH-treated cells, endogenous peroxidases and antioxidants such as glutathione may be rapidly recruited after the first hour, to scavenge H_2O_2 and $\cdot ONOO^-$ radicals.

At the early time point (20 min) that gave consistent and robust ROS/RNS signals after METH administration, the antioxidant NAC reduced the signal, which indicates that the fluorescent probe CM-H_2DCFDA was detecting ROS/RNS. Catalase and L-NMMA also decreased the METH-induced signal, which indicates that H_2O_2 and nitric oxide (NO) species were being generated. This result is consistent with the ability of METH to generate H_2O_2 and NO species from various sources, including dopamine oxidation and glutamate-induced NO synthase (NOS) activation (Krasnova and Cadet, 2009). It is interesting to note that the dose-response relationship of METH-induced reactive species generation did not follow a classic sigmoidal pattern, displaying greatest radical generation at the 3 μM concentration. This pattern of results is most likely attributable to multiple mechanisms and sources of METH-induced ROS/RNS generation (Krasnova and Cadet, 2009).

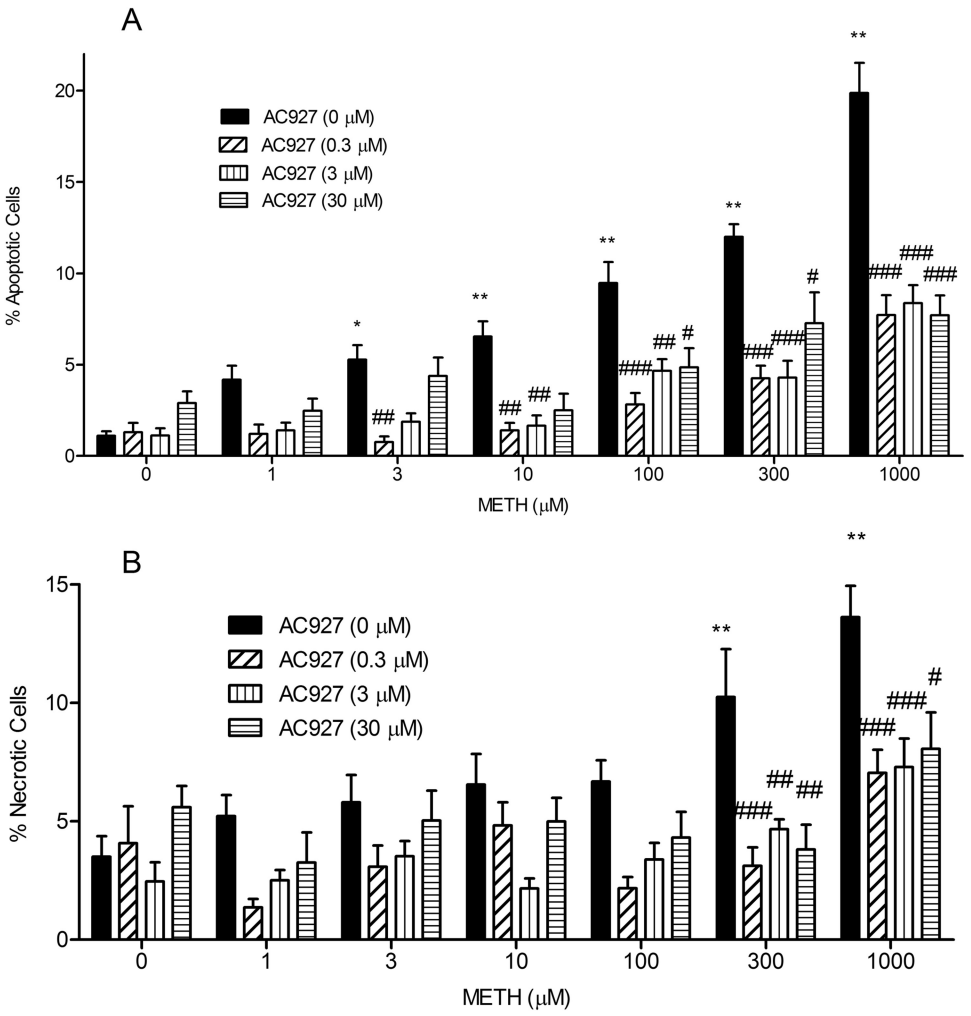

Fig. 6. AC927 protection against METH-induced apoptosis (A) and necrosis (B). NG108-15 cells were pretreated with AC927 (0–30 μM) before exposure to METH (0–1 mM) for 24 h. After 24 h, the wells were incubated with Hoechst 33342 and propidium iodide stains (20 μg/ml each), for determination of proportions of apoptotic and necrotic cells. Data represent the mean ± S.E.M. from two separate experiments ($n = 3$ per experiment). *, $p < 0.05$; **, $p < 0.01$, control versus METH-treated; #, $p < 0.05$; ##, $p < 0.01$; ###, $p < 0.001$, METH alone versus METH with AC927.

AC927 pretreatment attenuated the generation of ROS/RNS by METH. This effect of AC927 does not seem to be a general antioxidant effect, because AC927 did not prevent the H_2O_2-mediated ROS signal or reduce the basal cellular ROS/RNS signal. At the 4-h time point and beyond, however, AC927 (0.3 μM) attenuated basal cellular ROS/RNS levels and the ROS signal produced by $Na_2Cr_2O_7$. $Na_2Cr_2O_7$ generates $\cdot O_2^-$, H_2O_2, and $\cdot OH^-$ in cells (Azad et al., 2008). In combination with NO, $\cdot O_2^-$ can produce $\cdot ONOO^-$ in cells. The ability of AC927 to attenuate the ROS signal produced by $Na_2Cr_2O_7$ and not H_2O_2 is most likely attributable to increased levels of cellular antioxidant/antioxidant enzymes such as superoxide dismutase, which can reduce superoxide levels in the cell, or decreased levels of enzymes such as NOS, which can generate NO and lead to the production of $\cdot ONOO^-$. This effect of AC927 was observed after 4 h and not before, which suggests the induction of cellular antioxidants or a decrease in prooxidant/nitrosative stress enzymes, rather than an effect of generalized intrinsic antioxidant activity.

In agreement with this interpretation, several studies demonstrated the ability of σ receptors to modulate cellular ROS/RNS generation and antioxidant systems. Previous studies with tumor cells showed that σ_2 receptor activation causes ROS generation (Ostenfeld et al., 2005). σ_1 Receptors are involved in oxidative stress-mediated toxicities such as ischemic stroke and have been shown to provide protective effects (Schetz et al., 2007). σ Receptors also play a regulatory role in the redox state of cells and can modulate cellular NOS enzyme activity (Tsai et al., 2009; Yang et al., 2010). In addition to modulating the cellular redox system, σ receptors can regulate other systems that are involved in ROS/RNS generation by METH. First, σ receptors can regulate glutamate release through *N*-methyl-D-aspartate receptors, which causes neuronal NOS activation and nitrosative stress (DeCoster et al., 1995). Second, σ receptors can modulate microglial activation through Ca^{2+}-dependent mechanisms, which can contribute to the release of inflammatory cytokines and ROS/RNS generation (Hall et al., 2009). Third, σ receptors can regulate the release of dopamine, which undergoes autooxidation and is a major cause of METH-induced ROS generation (Gonzalez-Alvear and Werling, 1994; Derbez et al., 2002).

Although additional studies are needed to identify the specific mechanisms through which AC927 reduces the METH-induced generation of ROS/RNS, the studies reported here suggest that the modulation of dopamine release may be an important contributor. AC927 attenuates METH-induced dopamine release from NG108-15 cells; peak release was observed at the 3 μM concentration of METH, which is consistent with the peak observed in the ROS assay. Moreover, AC927 pretreatment prevented the dopamine release caused

by METH but not the nonspecific dopamine release caused by K^+-mediated hyperpolarization. This is consistent with the role of σ receptors in regulating DAT function and dopamine release in several in vivo and in vitro studies, including the involvement of Ca^{2+}-dependent and protein kinase C-mediated mechanisms (Booth and Baldessarini, 1991; Derbez et al., 2002). In addition to modulation of DAT function by σ receptors at lower concentrations, AC927 at higher concentrations may act in part as a DAT blocker in NG108-15 cells. The affinity of AC927 for DAT is 2939 ± 452 nM (Matsumoto et al., 2008). In addition, unpublished data suggest that AC927 at 1 μM can significantly attenuate dopamine uptake from rat synaptosomes (L. L. Werling, personal communication).

METH also caused apoptosis and necrosis in NG108-15 cells. Oxidative and nitrosative stress in cells can lead to the activation of pro-death pathways such as mitochondrial release of cytochrome *c* and/or caspase 3 activation, which ultimately leads to apoptotic or necrotic cell death (Higuchi et al., 1998). AC927 significantly attenuated both apoptotic and necrotic cell death, which is consistent with the role of σ receptors in cell death mechanisms (Bowen, 2000; Marrazzo et al., 2011). Furthermore, the protective effects of AC927 in NG108-15 cells are complementary and consistent with the neuroprotection observed in earlier in vivo studies (Matsumoto et al., 2008; Seminerio et al., 2011). In tumor cells, AC927 has been shown to prevent apoptosis caused by σ_2 receptor agonists, underscoring an important role of σ receptors in cell death mechanisms (Marrazzo et al., 2011).

Apart from σ receptors, D_1 receptor antagonism can protect against the apoptotic effects of METH (Jayanthi et al., 2005). Studies showed that σ_1 and D_1 receptors heteromerize in cells, which has implications for the downstream effects of psychostimulants, including the activation of adenyl cyclase and mitogen-activated protein kinase pathways (Navarro et al., 2010). AC927 may potentially modulate the σ_1 and D_1 receptor interaction and mitigate the toxic effects of METH.

In summary, our data demonstrate that METH can cause apoptosis and necrosis in an in vitro system representative of differentiated neuronal cells, which mechanistically involves dopamine release and induction of reactive oxygen/nitrogen radicals. A synthetic σ receptor ligand, AC927, can attenuate the cytotoxic effects of METH and contributing neurotoxic mechanisms. Future studies will be directed toward elucidation of the downstream neurotoxic pathways activated after ROS/RNS generation in differentiated NG108-15 cells. In addition, the individual contributions of the two subtypes of σ receptors will need to be distinguished, as better tools are developed.

Acknowledgments

We appreciate the expert technical advice of Dr. Kathy Brundage in the West Virginia University flow cytometry core facility. We also acknowledge Sudjit Luanpitpong for helping us to set up the apoptosis and necrosis assays.

Authorship Contributions

Participated in research design: Kaushal, Elliott, Robson, Iyer, Rojanasakul, and Matsumoto.

Conducted experiments: Kaushal, Elliott, and Robson.

Contributed new reagents or analytic tools: Coop.

Performed data analysis: Kaushal, Elliott, Robson, and Matsumoto.

Wrote or contributed to the writing of the manuscript: Kaushal, Elliott, Robson, Iyer, Rojanasakul, and Matsumoto.

References

Azad N, Iyer AK, Manosroi A, Wang L, and Rojanasakul Y (2008) Superoxide-mediated proteasomal degradation of Bcl-2 determines cell susceptibility to Cr(VI)-induced apoptosis. *Carcinogenesis* **29:**1538–1545.

Booth RG and Baldessarini RJ (1991) (+)-6,7-Benzomorphan sigma ligands stimulate dopamine synthesis in rat corpus striatum tissue. *Brain Res* **557:**349–352.

Bowen WD (2000) Sigma receptors: recent advances and new clinical potentials. *Pharm Acta Helv* **74:**211–218.

Cadet JL and Brannock C (1998) Free radicals and the pathobiology of brain dopamine systems. *Neurochem Int* **32:**117–131.

Cadet JL, Ordonez SV, and Ordonez JV (1997) Methamphetamine induces apoptosis in immortalized neural cells: protection by the proto-oncogene, bcl-2. *Synapse* **25:**176–184.

Cañete E and Diogène J (2008) Comparative study of the use of neuroblastoma cells (Neuro-2a) and neuroblastomaxglioma hybrid cells (NG108-15) for the toxic effect quantification of marine toxins. *Toxicon* **52:**541–550.

Crawford KW, Coop A, and Bowen WD (2002) σ_2 Receptors regulate changes in sphingolipid levels in breast tumor cells. *Eur J Pharmacol* **443:**207–209.

DeCoster MA, Klette KL, Knight ES, and Tortella FC (1995) Sigma receptor-mediated neuroprotection against glutamate toxicity in primary rat neuronal cultures. *Brain Res* **671:**45–53.

Derbez AE, Mody RM, and Werling LL (2002) σ_2-receptor regulation of dopamine transporter via activation of protein kinase C. *J Pharmacol Exp Ther* **301:**306–314.

Ghahary A, Vriend J, and Cheng KW (1989) Modification of the indolamine content in neuroblastoma × glioma hybrid NG108-15 cells upon induced differentiation. *Cell Mol Neurobiol* **9:**343–355.

Gonzalez-Alvear GM and Werling LL (1994) Regulation of [^{3}H]dopamine release from rat striatal slices by sigma receptor ligands. *J Pharmacol Exp Ther* **271:**212–219.

Guitart X, Codony X, and Monroy X (2004) Sigma receptors: biology and therapeutic potential. *Psychopharmacology (Berl)* **174:**301–319.

Hall AA, Herrera Y, Ajmo CT Jr, Cuevas J, and Pennypacker KR (2009) Sigma receptors suppress multiple aspects of microglial activation. *Glia* **57:**744–754.

Han DD and Gu HH (2006) Comparison of the monoamine transporters from human and mouse in their sensitivities to psychostimulant drugs. *BMC Pharmacol* **6:**6.

Hayashi T and Su TP (2003) Intracellular dynamics of sigma-1 receptors (σ_1 binding sites) in NG108-15 cells. *J Pharmacol Exp Ther* **306:**726–733.

Hayashi T and Su TP (2007) Sigma-1 receptor chaperones at the ER-mitochondrion interface regulate Ca^{2+} signaling and cell survival. *Cell* **131:**596–610.

Higuchi M, Honda T, Proske RJ, and Yeh ET (1998) Regulation of reactive oxygen species-induced apoptosis and necrosis by caspase 3-like proteases. *Oncogene* **17:**2753–2760.

Jayanthi S, Deng X, Ladenheim B, McCoy MT, Cluster A, Cai NS, and Cadet JL (2005) Calcineurin/NFAT-induced up-regulation of the Fas ligand/Fas death pathway is involved in methamphetamine-induced neuronal apoptosis. *Proc Natl Acad Sci USA* **102:**868–873.

Kekuda R, Prasad PD, Fei YJ, Leibach FH, and Ganapathy V (1996) Cloning and functional expression of the human type 1 sigma receptor (hSigmaR1). *Biochem Biophys Res Commun* **229:**553–558.

Krasnova IN and Cadet JL (2009) Methamphetamine toxicity and messengers of death. *Brain Res Rev* **60:**379–407.

Ma W, Pancrazio JJ, Coulombe M, Dumm J, Sathanoori R, Barker JL, Kowtha VC, Stenger DA, and Hickman JJ (1998) Neuronal and glial epitopes and transmitter-synthesizing enzymes appear in parallel with membrane excitability during neuroblastoma × glioma hybrid differentiation. *Brain Res Dev Brain Res* **106:**155–163.

Maeda DY, Williams W, Kim WE, Thatcher LN, Bowen WD, and Coop A (2002) *N*-arylalkylpiperidine as high-affinity sigma-1 and sigma-2 receptor ligands: phenylpropylamines as potential leads for selective sigma-2 agents. *Bioorg Med Chem Lett* **12:**497–500.

Marrazzo A, Fiorito J, Zappalà L, Prezzavento O, Ronsisvalle S, Pasquinucci L, Scoto GM, Bernardini R, and Ronsisvalle G (2011) Antiproliferative activity of phenylbutyrate ester of haloperidol metabolite II [(±)-MRJF4] in prostate cancer cells. *Eur J Med Chem* **46:**433–438.

Matsumoto RR, Shaikh J, Wilson LL, Vedam S, and Coop A (2008) Attenuation of methamphetamine-induced effects through the antagonism of sigma (σ) receptors: evidence from in vivo and in vitro studies. *Eur Neuropsychopharmacol* **18:**871–881.

McCann DJ, Weissman AD, and Su TP (1994) Sigma-1 and sigma-2 sites in rat brain: comparison of regional, ontogenetic, and subcellular patterns. *Synapse* **17:**182–189.

Melega WP, Jorgensen MJ, Laćan G, Way BM, Pham J, Morton G, Cho AK, and Fairbanks LA (2008) Long-term methamphetamine administration in the vervet monkey models aspects of a human exposure: brain neurotoxicity and behavioral profiles. *Neuropsychopharmacology* **33:**1441–1452.

Navarro G, Moreno E, Aymerich M, Marcellino D, McCormick PJ, Mallol J, Cortés A, Casadó V, Canela EI, Ortiz J, et al. (2010) Direct involvement of sigma-1 receptors in the dopamine D1 receptor-mediated effects of cocaine. *Proc Natl Acad Sci USA* **107:**18676–18681.

Nguyen EC, McCracken KA, Liu Y, Pouw B, and Matsumoto RR (2005) Involvement of sigma (σ) receptors in the acute actions of methamphetamine: receptor binding and behavioral studies. *Neuropharmacology* **49:**638–645.

O'Brien TJ, Ceryak S, and Patierno SR (2003) Complexities of chromium carcinogenesis: role of cellular response, repair and recovery mechanisms. *Mutat Res* **533:**3–36.

Ostenfeld MS, Fehrenbacher N, Høyer-Hansen M, Thomsen C, Farkas T, and Jäättelä M (2005) Effective tumor cell death by sigma-2 receptor ligand siramesine involves lysosomal leakage and oxidative stress. *Cancer Res* **65:**8975–8983.
Schetz JA, Perez E, Liu R, Chen S, Lee I, and Simpkins JW (2007) A prototypical sigma-1 receptor antagonist protects against brain ischemia. *Brain Res* **1181:**1–9.
Schmidt CJ and Lovenberg W (1985) In vitro demonstration of dopamine uptake by neostriatal serotonergic neurons of the rat. *Neurosci Lett* **59:**9–14.
Seminerio MJ, Kaushal N, Shaikh J, Huber JD, Coop A, and Matsumoto RR (2011) Sigma (σ) receptor ligand, AC927 (*N*-phenethylpiperidine oxalate), attenuates methamphetamine-induced hyperthermia and serotonin damage in mice. *Pharmacol Biochem Behav* **98:**12–20.
Su TP, Hayashi T, Maurice T, Buch S, and Ruoho AE (2010) The sigma-1 receptor chaperone as an inter-organelle signaling modulator. *Trends Pharmacol Sci* **31:**557–566.
Tsai SY, Hayashi T, Mori T, and Su TP (2009) Sigma-1 receptor chaperones and diseases. *Cent Nerv Syst Agents Med Chem* **9:**184–189.
Vilner BJ and Bowen WD (2000) Modulation of cellular calcium by sigma-2 receptors: release from intracellular stores in human SK-N-SH neuroblastoma cells. *J Pharmacol Exp Ther* **292:**900–911.
Vilner BJ, John CS, and Bowen WD (1995) Sigma-1 and sigma-2 receptors are expressed in a wide variety of human and rodent tumor cell lines. *Cancer Res* **55:**408–413.
Wheeler KT, Wang LM, Wallen CA, Childers SR, Cline JM, Keng PC, and Mach RH (2000) Sigma-2 receptors as a biomarker of proliferation in solid tumours. *Br J Cancer* **82:**1223–1232.
Wu CW, Ping YH, Yen JC, Chang CY, Wang SF, Yeh CL, Chi CW, and Lee HC (2007) Enhanced oxidative stress and aberrant mitochondrial biogenesis in human neuroblastoma SH-SY5Y cells during methamphetamine induced apoptosis. *Toxicol Appl Pharmacol* **220:**243–251.
Yang ZJ, Carter EL, Torbey MT, Martin LJ, and Koehler RC (2010) Sigma receptor ligand 4-phenyl-1-(4-phenylbutyl)-piperidine modulates neuronal nitric oxide synthase/postsynaptic density-95 coupling mechanisms and protects against neonatal ischemic degeneration of striatal neurons. *Exp Neurol* **221:**166–174.
Zeng C, Vangveravong S, Xu J, Chang KC, Hotchkiss RS, Wheeler KT, Shen D, Zhuang ZP, Kung HF, and Mach RH (2007) Subcellular localization of sigma-2 receptors in breast cancer cells using two-photon and confocal microscopy. *Cancer Res* **67:**6708–6716.

Address correspondence to: Dr. Rae R. Matsumoto, West Virginia University, School of Pharmacy, P.O. Box 9500, Morgantown, WV 26506. E-mail: rmatsumoto@hsc.wvu.edu